Downloaded from genome.cshlp.org on August 3, 2026 . Published by Cold Spring Harbor Laboratory Press

A comparison of ancient DNA yields across ossicles and the petrous bone reveals the best preservation in the stapes and incus

Ekin Saglican, Arda Sevkar, Duygu Deniz Kazanci, et al.

Genome Res. published online June 11, 2026
Access the most recent version at doi:10.1101/gr.281213.125

P<P Published online June 11, 2026 in advance of the print journal.

Creative Commons License This article is distributed exclusively by Cold Spring Harbor Laboratory Press for the first six months after the full-issue publication date (see https://genome.cshlp.org/site/misc/terms.xhtml). After six months, it is available under a Creative Commons License (Attribution-NonCommercial 4.0 International), as described at http://creativecommons.org/licenses/by-nc/4.0/.

Email Alerting Service Receive free email alerts when new articles cite this article - sign up in the box at the top right corner of the article or **click here.**

Advance online articles have been peer reviewed and accepted for publication but have not yet appeared in the paper journal (edited, typeset versions may be posted when available prior to final publication). Advance online articles are citable and establish publication priority; they are indexed by PubMed from initial publication. Citations to Advance online articles must include the digital object identifier (DOIs) and date of initial publication.

To subscribe to *Genome Research* go to:
https://genome.cshlp.org/subscriptions

© 2026 Saglican et al.; Published by Cold Spring Harbor Laboratory Press

Downloaded from genome.cshlp.org on August 3, 2026 . Published by Cold Spring Harbor Laboratory Press

Method

A comparison of ancient DNA yields across ossicles and the petrous bone reveals the best preservation in the stapes and incus

Ekin Sağlıcan,[1,13] Arda Sevkar,[2,13] Duygu Deniz Kazancı,[2,3] Gonzalo Oteo-García,[4,5,6] Sevgi Yorulmaz,[3] Kıvılcım Başak Vural,[3] Gökhan Çakan,[2] Gökçen Adiloğlu,[2] Duru Buldak,[3] Güneş Duru,[7] Aliye Öztan,[8] Brenna Hassett,[9] Nurcan Kayacan,[10] Aslı Erim Özdoğan,[11] Anders Götherström,[5,6] Füsun Özer,[2] Ömür Dilek Erdal,[2] Yılmaz Selim Erdal,[2] and Mehmet Somel[3,5,12]

[1]*Graduate School of Informatics, Middle East Technical University, 06800 Ankara, Türkiye;* [2]*Department of Anthropology, Hacettepe University, 06800 Ankara, Türkiye;* [3]*Department of Biological Sciences, Middle East Technical University, 06800 Ankara, Türkiye;* [4]*Dipartimento di Biologia Ambientale, Sapienza Università di Roma, 00185 Rome, Italy;* [5]*Center for Palaeogenetics, Stockholm University, SE-106 91 Stockholm, Sweden;* [6]*Department of Archaeology and Classical Studies, Stockholm University, SE-106 91 Stockholm, Sweden;* [7]*Department of Archaeology, Mimar Sinan Fine Arts University, 34381 Şişli/İstanbul, Türkiye;* [8]*Archaeology Department, Ankara University, 06100 Ankara, Türkiye;* [9]*School of Law and Policing, University of Lancashire, Preston PR1 2UQ, United Kingdom;* [10]*Prehistory Department, Faculty of Letters, Istanbul University, 34459 Istanbul, Türkiye;* [11]*Department of Archaeology, Çanakkale Onsekiz Mart University, 17100 Çanakkale, Türkiye;* [12]*Swedish Collegium for Advanced Study, SE-752 36 Uppsala, Sweden*

The petrous bone is considered the most efficient source of endogenous DNA across skeletal tissues in ancient DNA (aDNA) research as well as in forensic work. Recently, aDNA in auditory ossicle bones was shown to be comparably well preserved as in the petrous, although no attempt was made to distinguish among the three ossicle bones. In this study, we compare aDNA profiles across matched ossicle- and petrous-derived sequencing libraries prepared from 29 human skeletons from Neolithic Anatolia and Medieval Iberia. We find that the stapes and incus provide higher human endogenous aDNA than the petrous bone, with >2× higher median rates of endogenous aDNA recovery, whereas the malleus performs similarly to the petrous. Human aDNA fragments retrieved from the stapes were 8% longer than those from the petrous, whereas postmortem damage, clonality, and contamination rates were comparable among the studied bone types. These observations are corroborated by data from nonmatched ossicle or petrous libraries from 81 individuals from the same contexts, with the highest endogenous aDNA content observed in the stapes. Despite being the smallest bone in the human skeleton, the stapes, along with the incus, may be among the most optimal aDNA sources yet identified.

[Supplemental material is available for this article.]

The efficient retrieval of postmortem or ancient DNA (aDNA) from archaeological and historical human skeletal remains is a major limiting factor in paleogenomics and forensic genetics. Over the past decade, the petrous bone has been recognized as the most effective source in both archaeological and forensic settings (Gamba et al. 2014; Pinhasi et al. 2015, 2019; Gaudio et al. 2019). Endogenous human DNA preservation in the petrous bone (and more specifically, the osseous labyrinth, or the otic capsule, which includes the cochlea) tends to be better than in other skeletal elements, including long bones (femur, tibia, etc.), phalanges, teeth, calcaneus, and the talus (Parker et al. 2020; Hofreiter et al. 2021; Haarkötter et al. 2023; Zupanič Pajnič et al. 2025). This property is attributed to limited bone remodeling that occurs during the lifetime and a high concentration of osteocytes in the petrous (Pinhasi et al. 2015; Ibrahim et al. 2022).

Before the discovery of the petrous bone as an effective human aDNA source, Bell and colleagues (2008) had suggested that ear ossicles, which contain a high proportion of mineralized osteocytes, could be an optimal target for DNA and protein retrieval from postmortem material. More recently, Sirak et al. (2020) compared aDNA yields in ossicles and petrous bone from 10 human skeletons by shotgun sequencing. These authors found (1) similar endogenous DNA content in ossicles as in the petrous bone (with nonsignificantly higher levels in ossicles), (2) slightly lower DNA postmortem damage (PMD; in the form of cytosine deamination) in ossicles, (3) three times higher human contamination in ossicles

[13]**These authors contributed equally to this work.**
Corresponding authors: quetzalekin@gmail.com, sevkararda@gmail.com, somelmehmet@gmail.com
Article published online before print. Article, supplemental material, and publication date are at https://www.genome.org/cgi/doi/10.1101/gr.281213.125.

© 2026 Sağlıcan et al. This article is distributed exclusively by Cold Spring Harbor Laboratory Press for the first six months after the full-issue publication date (see https://genome.cshlp.org/site/misc/terms.xhtml). After six months, it is available under a Creative Commons License (Attribution-NonCommercial 4.0 International), as described at http://creativecommons.org/licenses/by-nc/4.0/.

Downloaded from genome.cshlp.org on August 3, 2026 . Published by Cold Spring Harbor Laboratory Press

(even though all the libraries studied had <5% contamination levels), and (4) similar levels of library complexity.

Sirak and colleagues (2020) thus concluded that ossicle bones could be a useful source of aDNA, especially when the petrous bone is not accessible and/or when its destructive sampling is undesirable, as its morphology can be used for studying genetic relationships (Ponce de León et al. 2018). Several paleogenomic and forensic genetic studies have also included ossicles as a DNA source, although with limited sample sizes and/or without comparison with the petrous bone (Schwark et al. 2015; Prendergast et al. 2019). Meanwhile, no study, to the best of our knowledge, attempted to differentiate between the three different auditory ossicle elements: the stapes (stirrup), malleus (hammer), and incus (anvil). These three bones might be expected to differ in DNA preservation levels given the differences in their developmental profiles and in their bone and osteocyte densities (Marotti et al. 1998; Richard et al. 2017; Ivanovic et al. 2024).

Results

We compared aDNA sequencing libraries obtained from 29 archaeological skeletons with both petrous and ossicle tissue, including nine stapes, nine malleus, eight incus, and four unidentified ossicle fragments (Methods). The skeletons included adults and subadults and derive from four archaeological excavation sites from across ancient Central Anatolia and Upper Mesopotamia, ranging from around 11,000 before present (BP) to 7000 BP and covering mainly temperate steppe-like environments, and from two sites in Iberia dated to the Medieval period (eighth to thirteenth century CE) (Supplemental Table S1). Ossicles were collected from temporal bones that had not been washed (a widespread procedure applied in skeletal anthropology laboratories to clean excavated bones with water, which can cause the loss of ossicles) (for representative ossicle bones, see Fig. 1).

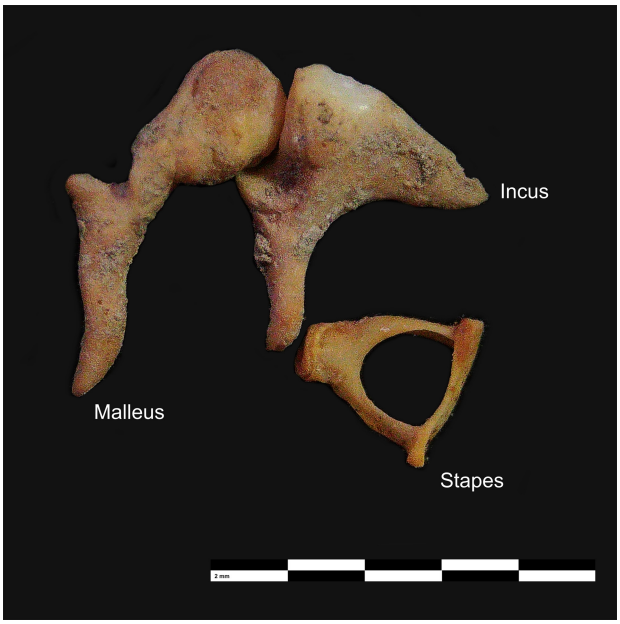

Figure 1. Representative auditory ossicle bones used in this study. Each black and white segment in the scale bar represents 2 mm.

We removed soil deposits within ear canals, which occasionally revealed ossicle bones (for information about retrieval methods and frequencies, see the Discussion and Methods). When multiple ossicle elements were present, we randomly chose one ossicle bone, except for one individual (Ind078), who was sampled for both malleus and incus (Methods) (Table 1; Supplemental Table S1). We additionally expanded our data set with 81 unmatched ossicle- or petrous-derived libraries from the same site (site 7), including five stapes, four malleus, and two incus fragments and one unidentified ossicle fragment without matching petrous libraries, as well as 69 petrous-derived libraries without matching ossicle libraries (Table 1; Supplemental Table S1). We further used five petrous-matched tooth libraries from Neolithic to Early Modern contexts in Anatolia for microbial content analyses (Methods) (Supplemental Table S1).

The ossicles were dissolved directly in the lysis buffer, whereas the petrous bone samples were pulverized by drilling, and DNA was extracted using the Dabney protocol (Methods) (Dabney et al. 2013). We constructed double-stranded Illumina libraries using the Dabney extraction (Dabney et al. 2013) and Meyer–Kircher library preparation protocols (Meyer and Kircher 2010) for the 122 libraries from Anatolia and constructed single-stranded libraries using the Santa Cruz method (Kapp et al. 2021) for the 26 libraries from Iberia. We shotgun sequenced each library once between ~0.8 million and 80 million reads (median ~11.5 million). To standardize comparisons, libraries exceeding 1 million total reads were downsampled to a 1-million-read threshold (Methods) (Supplemental Table S1). We mapped the data to the human reference genome (GRCh37) and compared various characteristics of the ossicle bone– and petrous bone–based libraries (Methods): endogenous human DNA proportion, human fragment length, PMD, clonality, and contamination. We also compared the microbial content in terms of possible sources, namely, human, oral microbiome, and environmental microbes, to characterize the microbial profile of each tissue type, which we also compared with five teeth libraries (Methods).

Endogenous human DNA proportion, the most direct indicator of ancient human DNA preservation, was calculated as the fraction of reads mapping to the human genome (without removing duplicates). Across the combined set of 30 ossicle-based versus petrous-based libraries, there was a visible and significant increase in endogenous human DNA in the former (Wilcoxon signed-rank test [WSR] test $P < 0.001$). This effect was mainly observed for the stapes and incus (Fig. 2A). In nine petrous-stapes comparisons, we found a median gain of ~110% in the stapes (WSR test $P = 0.027$). In seven out of nine comparisons, the stapes had higher endogenous DNA; only in a single individual did we observe a visibly lower yield in the stapes than in the petrous, and in one case, the petrous and stapes had equally high (~70%) endogenous DNA. In the petrous–incus comparisons ($n = 8$), we observed an increase in human endogenous DNA values in all cases, with a median increase of ~380% (WSR test $P = 0.008$). Among the malleus–petrous comparisons, seven in nine cases revealed slightly higher endogenous human DNA than the petrous, although there was no significant effect (median increase ~32%; WSR test $P = 0.20$) (Fig. 2A).

We further compared DNA content across all 140 ossicle- and petrous-derived libraries in our expanded data set (14 stapes, 13 malleus, 10 incus, five unidentified ossicle, and 98 petrous, belonging to either the same or to different individuals). In these unmatched comparisons, we found significantly better human DNA preservation in the stapes than in all other studied tissues (Mann–Whitney *U* [MWU] test with Benjamini–Hochberg adjustment for

Downloaded from genome.cshlp.org on August 3, 2026 . Published by Cold Spring Harbor Laboratory Press

Table 1. Number of libraries and individuals used

Experimental design	Tissue combination	Number of libraries	Number of individuals
Matched petrous-ossicle samples	P, S	18	9
	P, M	16	8
	P, I	14	7
	P, M, I	3	1
	P, UIO	8	4
	Total	59	29
Unmatched samples	P	69	69
	S	5	5
	M	4	4
	I	2	2
	UIO	1	1
	Total	81	81

Matched petrous-ossicle samples refers to cases in which we collected one petrous and one ossicle type per individual (except for a single case, Ind078, for which we generated libraries for both malleus and incus from the same skeleton). Unmatched samples refers to cases in which an individual was represented by either a petrous- or ossicle-derived library. (P) Petrous, (S) stapes, (M) malleus, (I) incus, and (UIO) unidentified ossicle. The unidentified category includes ossicles in which the type had not been recorded or ossicles that were fragmented so that morphological identification was not possible. The table does not include five tooth-derived and three matched petrous-derived libraries used in microbial comparisons (two of the tooth-derived libraries have matched petrous and ossicle samples represented in the table). For details of the libraries, see Supplemental Table S1.

multiple testing, $P_{adj} < 0.001$). The incus had the second best preservation in these unmatched comparisons, with significantly higher values than in the malleus and petrous (MWU test $P_{adj} < 0.05$) (Fig. 3A). To control for variability among archaeological sites in this expanded data set, we restricted the analysis to libraries derived from subadult skeletons interred in the Neolithic/Chalcolithic levels of site 7 (11 stapes, eight malleus, four incus, one unidentified ossicle, and 80 petrous libraries). We again found superior performance of the stapes compared with both the petrous and malleus (MWU test $P_{adj} < 0.05$) (Fig. 3D). We then asked whether the observed differences could reflect a pattern in which the stapes is retrieved only in highly preserved temporal bones but is lost in low-preserved ones, creating an artificial signal of higher endogenous DNA in the stapes in unmatched comparisons. To test this, we limited comparisons to libraries with human proportion values ≥25% in both the petrous ($n = 28$) and the stapes ($n = 10$). We again observed higher endogenous DNA proportions in the stapes compared with petrous libraries (MWU test $P_{adj} < 0.001$) (Fig. 3D). The same comparisons involving the incus versus petrous bones were not statistically significant, likely owing to the limited number of incus specimens ($n = 4$ and 3, respectively).

Human DNA fragment length is another indicator of DNA preservation. Fragment lengths in the nine stapes-derived libraries were, on average, significantly longer (mean +5.1 bp) than in the matched petrous-derived ones (WSR test $P = 0.01$) (Fig. 2B). There was no significant difference between the eight matched incus- and petrous-derived libraries (WSR test $P > 0.05$), whereas fragment lengths in the nine malleus-derived libraries were on average slightly shorter (mean −4.3 bp) than in the matched petrous-derived ones (WSR test $P = 0.01$) (Fig. 2B). Across the set of all 140 ossicle and petrous libraries (matched and unmatched), we found trends toward longer fragments (mean +5.6 bp) in the stapes and toward shorter fragments in the malleus and incus (means −3.3 bp and −5.4 bp, respectively) compared with the petrous, but none were significant (MWU test $P_{adj} > 0.05$) (Fig. 3B). A similar pattern was observed when the analysis was restricted to site 7 individuals across varying human proportion thresholds, with no significant differences between the ossicle and petrous libraries (MWU test $P_{adj} > 0.05$) (Fig. 3E).

We next studied PMD, estimated as cytosine deamination–caused C-to-T mismatches on fragment ends. We found similar PMD levels between ossicles and matched petrous libraries for each ossicle type, as well as no significant difference in comparisons involving all 140 libraries or in analysis restricted to site 7 individuals at varying human proportion thresholds (WSR test $P > 0.05$) (Figs. 2C, 3C–F).

Sirak and colleagues (2020) had reported slightly but nonsignificantly higher clonality (inverse of library complexity) and also significantly higher contamination levels in their ossicle libraries compared with their petrous libraries. We measured clonality as the proportion of duplicate reads within each discrete library. Clonalities of ossicle-derived libraries were similar to those of matched petrous ones, with no significant difference (WSR test $P > 0.05$) (Fig. 2D). We further studied human contamination estimates using the *contamMix* method (Fu et al. 2013), limiting the analysis to 18 matched pairs with at least 1× mitochondrial DNA coverage (Methods). We found no significant difference in human contamination levels between ossicle- and petrous-based libraries (WSR test $P > 0.05$) (Fig. 2E).

Finally, we analyzed the microbial content of the studied petrous and ossicle samples, as well as five tooth cementum libraries and three matched petrous libraries included for this comparison (Supplemental Table S2). We assigned reads to microbial taxa using KrakenUniq (Breitwieser et al. 2018) and further divided these into oral and nonoral categories using several databases (Methods). A small fraction of reads was assigned to oral microbes in teeth libraries (median 0.22%) and practically none in petrous and ossicle libraries (median 0%–0%) (Supplemental Fig. 1A). Teeth also had the highest proportions of reads assigned to nonoral microbes (median 2.3%) (Supplemental Fig. 1B), which include environmental taxa (e.g., soil and aquatic microorganisms associated with postmortem decomposition and taphonomic processes) and potential laboratory contaminants. Petrous libraries ranked second (median 0.32%), whereas ossicle libraries again contained practically no reads assigned to nonoral microbes (~0.01%) (Supplemental Fig. 1B). These rates were significantly lower for the stapes and incus compared with either the teeth or the petrous (MWU test $P_{adj} < 0.05$).

Discussion

Sirak et al. (2020) had previously suggested that ossicles could be used as an alternative to the petrous bone as an efficient aDNA source. Our results now indicate the stapes, and likely the incus, as a significantly better source of human aDNA than the petrous and the malleus. This quality is reflected not only in higher endogenous DNA proportion (for the stapes and incus) but also in the longer DNA fragments (for the stapes). This would potentially elevate the stapes to the top of the list of human skeletal elements for ancient and forensic DNA retrieval.

Our conclusions are subject to a number of limitations. First, we could not conduct within-individual comparisons across the

Downloaded from genome.cshlp.org on August 3, 2026 . Published by Cold Spring Harbor Laboratory Press

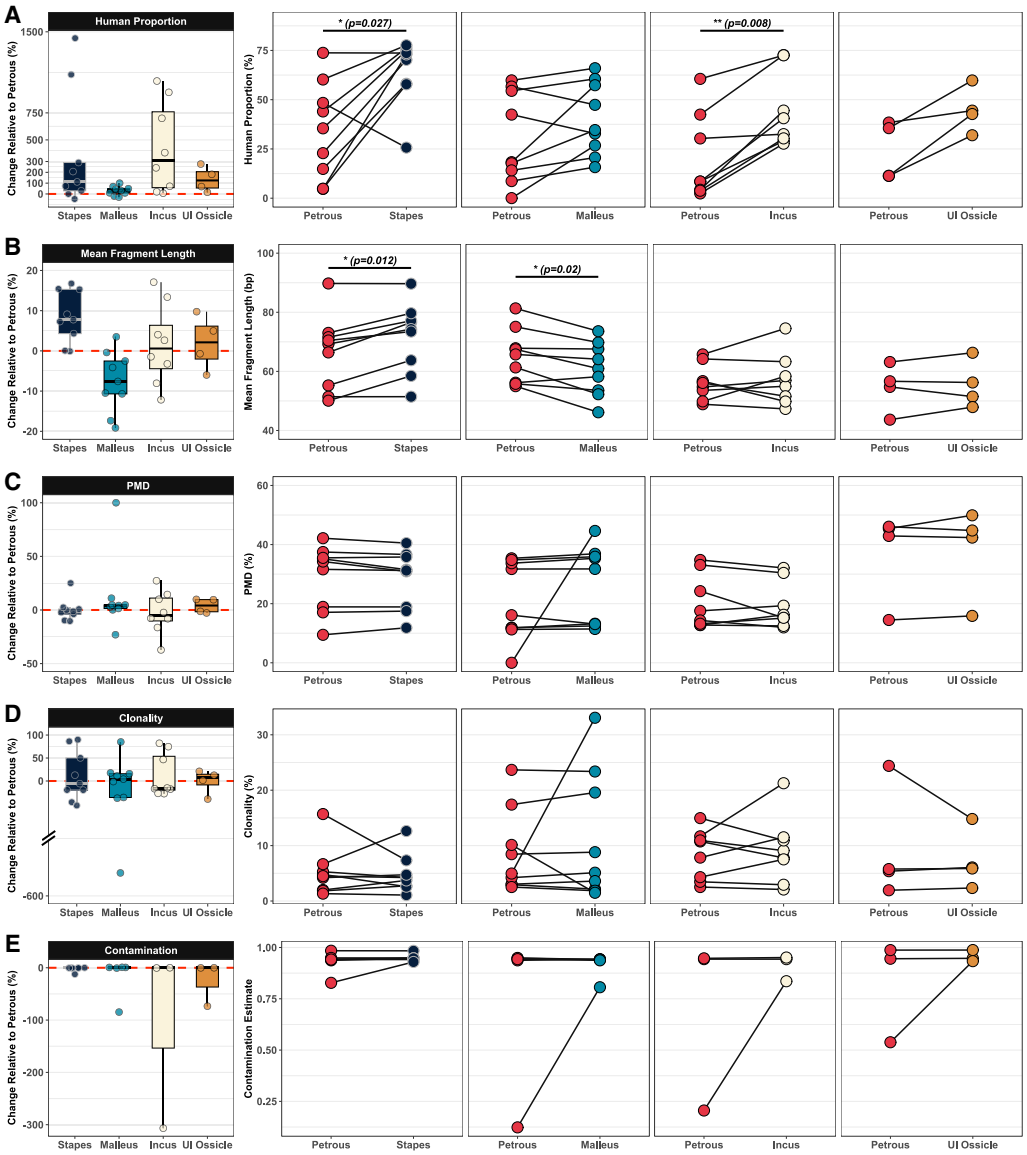

Figure 2. Comparison of the mapping statistics in matched shotgun DNA libraries prepared from each ossicle type relative to those prepared from the petrous bone: (*A*) Comparison of human proportions, (*B*) comparison of mean fragment lengths, (*C*) comparison of deamination values (postmortem damage [PMD]), (*D*) comparison of clonality values. (*E*) Contamination was estimated using the contamMix method (Fu et al. 2013), including only matched libraries with >1× mtDNA coverage. Only statistically significant Wilcoxon signed-rank (WSR) test results are shown: (*) $P_{adj} < 0.05$, (**) $P_{adj} < 0.01$, (***) $P_{adj} < 0.001$. (UI Ossicle) Unidentified ossicle.

three ossicle types, as nearly all our petrous-matched samples consisted of one randomly sampled ossicle bone per individual. Meanwhile, both the overall endogenous DNA content (Fig. 3A, D), as well as the improvement of the endogenous DNA content relative to the petrous (Fig. 2A), indirectly support higher performance of the stapes and the incus over the malleus. In the single case in which we could study both the malleus and incus from the same individual (Ind078), the incus had >2× higher endogenous content (33% vs. 73%, respectively), in line with the indirect comparisons.

The availability of the ossicles from skeletal collections and preservation biases poses another question. In our preliminary records, the relative frequency of ossicle detection varies significantly among sample sets. Across 566 Anatolian skeletons studied (DD Kazancı, pers. comm.) spanning the last 10,000 years, we recorded at least one ossicle (without distinguishing between types) in 52 instances (9%). Notably, the majority of these skeletons were washed to various degrees, and the lowest frequency was recorded in the Neolithic period (around 9000–6000 BCE) Anatolian sample (four in 147). In the Medieval Iberian sample, which was also heterogeneous with respect to the cleaning state and included 70 petrous bones (G Oteo-García, pers. comm.), we identified at least one ossicle 48 times (69%); the retrieval frequency again seemed to be inversely related to the petrous bone being washed. These figures are compatible with the reported ossicle retrieval frequencies in the literature, ranging from 4% to 53% in diverse collections (Sakalinskas and Jankauskas 1991; Bruintjes et al. 1997; Qvist 2000). This variation in ossicle retrieval is partly

Downloaded from genome.cshlp.org on August 3, 2026 . Published by Cold Spring Harbor Laboratory Press

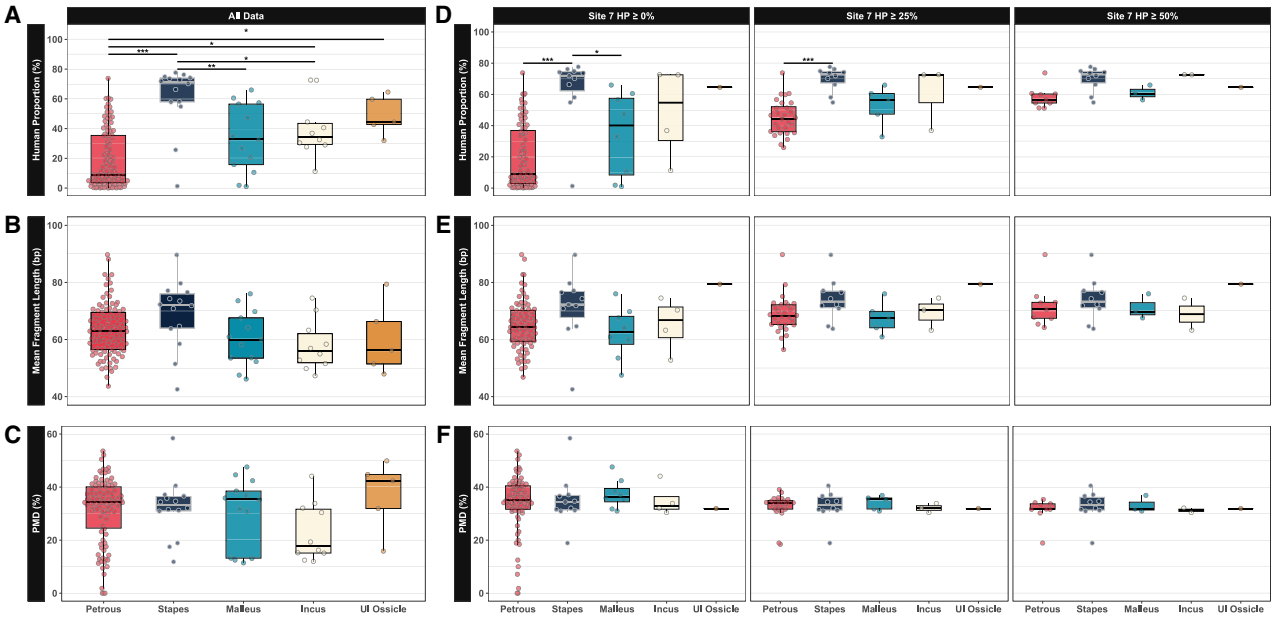

Figure 3. Comparison of mapping statistics in the expanded data set. (*A*–C) Mapping statistics for all 140 ossicle- and petrous-derived libraries. (*D*–*F*) Mapping statistics for libraries prepared from subadult individuals recovered from the Neolithic/Chalcolithic levels of Anatolian site 7 ($n = 92$). Mann–Whitney *U* test results are indicated *above* the plots. Only statistically significant comparisons are shown: (***) $P_{adj} < 0.001$, (**) $P_{adj} < 0.01$, (*) $P_{adj} < 0.05$. (PMD) Postmortem damage, (HP) Endogenous human DNA proportion.

attributable to care in excavation, storage, and processing (Qvist 2000), including whether washing is applied or not. Taphonomic processes likely also play a role, reflected in the high (>50%) ossicle retrieval frequencies reported for Medieval Iberia and Denmark (this study and that of Qvist 2000, respectively). In addition, in four publications reporting ossicle retrieval, the stapes was found at lower frequencies (30%–50%) relative to the incus and malleus (Lisoněk et al. 1986; Sakalinskas and Jankauskas 1991; Bruintjes et al. 1997; Qvist 2000). Qvist (2000) suggested the difference could represent the erosion of the stapes during lifetime. Such age-related fragility could also explain why most of the stapes samples in our study derived from Anatolian site 7, which was dominated by newborns (Supplemental Table S1). It is further possible that ossicles and especially the stapes are often found when the overall skeletal preservation is good. An observation that supports a preservation bias is that in our sample from site 7, nonmatched petrous libraries ($n = 69$) have much lower endogenous DNA proportions compared with the matched petrous libraries in which ossicles were identified ($n = 11$): median 7% versus 54%. We remind, however, that even among highly preserved samples, the stapes had better DNA yields compared with the petrous. Future work systematically documenting the frequency of ossicle retrieval in diverse settings and among carefully handled crania, including the frequency in which they might be found in both left and right temporal bones, could help further assess the potential of the use of ossicles as an aDNA source.

Another potential limitation of our study involves the efficiency of petrous bone sampling. We extracted DNA from the petrous bone by drilling into the otic capsule and mainly targeting the cochlea, but we frequently also drilled the vestibule and semicircular canals in order to collect additional power. This may have introduced variability in aDNA retrieval, as the cochlea is considered the densest element (Pinhasi et al. 2015) and the heat caused by drilling (even though generally performed at low speeds) could degrade biomolecules. The protocol Sirak et al. (2020) adopted in their petrous versus ossicle comparison was more targeted, in which the authors isolated the cochlea using a sandblaster and powdered the bone with a freezer mill (Pinhasi et al. 2019). This latter approach is possibly more efficient in retrieving aDNA from the petrous bone and might partly explain why we observe improved rates with ossicles over the petrous, whereas Sirak and colleagues found comparable rates. However, this likely does not explain all our findings because we also observe differences among the ossicle types. For instance, we find that the endogenous DNA proportions in the malleus are comparable to those in the petrous, similar to what Sirak et al. (2020) report for ossicles in general, and they are lower than those of the stapes and incus. Further, human aDNA fragments in the stapes tend to be longer than in other tissues. Considering that our ossicle processing approach, dissolving in an incubation buffer, is the same as that of Sirak and colleagues, the higher performance of the stapes relative to the petrous bone and the malleus is unlikely to be fully explained by petrous drilling.

Finally, we did not include teeth in our paired comparisons of endogenous proportion. Previous reports have found the tooth cementum to perform either similar to the petrous bone (Hansen et al. 2017) or slightly worse (Parker et al. 2020) in terms of human DNA preservation. We can thus infer that the stapes and incus would have higher endogenous DNA yields than the cementum. Meanwhile, teeth samples have the advantage of carrying information about commensal and pathogenic microbes of diverse origin compared with the petrous bone (Sikora et al. 2025). Our analyses suggest that the ossicles may carry even lower amounts of microbial DNA than the petrous and would not be a useful resource for metagenomic analyses.

The ossicle bones are known to undergo only limited remodeling after 1–2 years of age (Marotti et al. 1998; Rolvien et al. 2018), a pattern also observed in the petrous bone (Sørensen et al. 1992;

Downloaded from genome.cshlp.org on August 3, 2026 . Published by Cold Spring Harbor Laboratory Press

Frisch et al. 1998). Sirak and colleagues (2020) argued that this limited bone remodeling could explain comparable DNA preservation levels in ossicle and petrous samples. In the absence of remodeling, mineralized, apoptotic-like osteocytes with condensed chromatin structures are reported to accumulate in ossicles (Bell et al. 2008; Rolvien et al. 2018), which could be the source of preserved aDNA. Our microbial analyses also imply that the ossicles may be generally more resistant to microbial colonization than the petrous and tooth. The reason for the relatively good DNA preservation in the stapes (and possibly the incus) over the malleus is yet unclear. Several studies have reported differences in histology and development among ossicles, including the later ossification of the stapes compared to the malleus and incus (Richard et al. 2017), high bone density in the stapes footplate (Ivanovic et al. 2024), a higher percentage of dead osteocytes in the stapes compared with the other ossicles through lifetime (Marotti et al. 1998), and increasing fragility with age (Qvist 2000). Such differences could possibly contribute to differential survival of bone structure and of DNA among the ossicles.

Our work indicates that the stapes, with its small size (~3–6 mm) and fragile appearance, is an exceptionally preserved bone element. Despite its relatively limited survivorship, whenever retrieved, it can be a superior source of human aDNA over the petrous as well as other human bone elements. The incus may also be a comparably good source, at least with respect to endogenous DNA proportions. Relative to petrous sampling, the ossicles have the additional advantage of being amenable to collection for aDNA analysis without destruction to the temporal bone. Meanwhile, the ossicles also have a unique role in bioarcheology because they can be used to study maternal diet during pregnancy through stable isotopes (because of their low postnatal remodeling). However, the stapes has been noted as being too small for sufficient collagen extraction for dietary analysis (Leskovar et al. 2019). Sampling the stapes for aDNA analysis therefore appears a reasonable choice, notwithstanding the two constraints mentioned earlier: its relatively bad preservation (compared with the petrous bone) and its lack of metagenomic information about commensal or pathogenic microbes (compared with teeth) (Margaryan et al. 2018; Sikora et al. 2025). Beyond these limitations, the stapes could become a main target tissue for archeogenomic studies and also in forensic analyses (Zupanič Pajnič et al. 2025).

We thus echo the call by Sirak and colleagues to the archaeology and bioarcheology communities to treat skull fragments carefully to avoid the loss of ossicles during excavation and to refrain from washing temporal bones before sampling ossicles. For ossicle retrieval protocol from archaeological skeletons, see the Methods section.

Methods

All experiments were conducted in dedicated aDNA laboratories at Middle East Technical University and Hacettepe University in Ankara, Türkiye, and at the Center for Paleogenetics of Stockholm University, Sweden. Anatolian skeletal material was processed in Ankara and Iberian material in Stockholm. Experiments were performed by five researchers (for list, see Supplemental Table S1).

Three features of the experimental design limit possible confounding between biological and technical artifacts: (1) our main observations were based on matched comparisons between ossicle- versus petrous-derived libraries; (2) in matched comparisons, we used the same set of reagents for the petrous and the ossicle libraries; and (3) in unmatched comparisons, the bulk of the ossicle and petrous libraries derived from a single archaeological context (104 in 140, Anatolian site 7) and were produced by a single researcher with the same reagents (produced within 08/2021-07/2022), allowing us to perform unmatched comparisons using only this data subset.

Several precautionary measures were taken to minimize the risk of contamination during the experiments. All equipment, utensils, and laboratory surfaces were decontaminated with DNA AWAY (Thermo Fisher Scientific) or a bleach solution before each use and in-between different samples. All solutions not sensitive to UV light were exposed to UV-irradiation for 30 min in a UV cross-linker. Negative controls were included at every step necessary to monitor potential contamination.

Sample preparation

Ossicle sampling

Ossicles were collected from temporal bones in which the middle ear had not been fully cleaned by washing. The procedure requires careful handling as outlined in a video protocol (dx.doi.org/10.17504/protocols.io.kxygx42zol8j/v1). Briefly, soil deposits in the ear canals were removed with cotton swabs and/or picks, using distilled water depending on the soil consistency, which occasionally revealed ossicles dislodged in the process. Sometimes, we also found the stapes fallen into the window opening leading to the vestibule. From ossicles collected in this manner from each temporal bone, we randomly selected one element (except for Ind078 sampled for both the malleus and incus). We analyzed only one temporal bone per individual such that the petrous and the ossicle samples derived from the same side, right or left. A small number of samples collected in the early stages of the experimental work when we had not started recording the ossicle type and a few cases in which the ossicles were too fragmented to preclude identification were collectively labeled as "unidentified ossicle." In Ankara, the ossicle bones retrieved were used directly in the following steps, whereas in Stockholm, they were decontaminated when soil deposits were present on the bone surface by wiping with cotton swabs soaked in 1% bleach solution followed by rinsing with distilled water.

Petrous sampling

Ear canals within the petrous bones were cleaned both mechanically and chemically when extensive soil deposits were present. Mechanical cleaning involved removing the outer layer of the ear canal using Dremel tools with a sterile tip, whereas for chemical cleaning, we used 1% bleach solution followed by rinsing with sterile water.

From the petrous bone (otic capsule) material, we obtained ~20–80 mg of bone powder by drilling into surface-cleaned bones with a Dremel 3000 or Dremel Fortiflex 9100-21. The drilling targeted the otic capsule, which primarily includes the majority of the vestibule; however, the semicircular canals and cochlea were also occasionally included in order to collect sufficient powder from the petrous bone. In experiments performed in Ankara, the drilling was performed at the lowest speed (~5000 RPM for the Dremel 3000 and near zero for the Dremel Fortiflex 9100-21) with minimal contact time to reduce heat. In experiments performed in Stockholm, drilling was performed at medium speed.

Tooth sampling

The tooth samples used in this study date to Neolithic, Medieval, and Early Modern contexts from Anatolia (Supplemental Table

Downloaded from genome.cshlp.org on August 3, 2026 . Published by Cold Spring Harbor Laboratory Press

S1). Molar teeth that were intact within the mandible or maxilla were used in this study. In the first step, teeth were removed from the alveolar bone and cleaned with distilled water using cotton swabs or towels if needed. Subsequently, the pulp cavity was drilled at the level of the cementoenamel junction using a Dremel tool as described for petrous bone sampling.

Experimental procedures

DNA extraction

We used a modified protocol based on the work of Dabney et al. (2013) for aDNA extraction. The auditory ossicle bones were directly added to the lysis buffer, without pulverizing or additional cleaning. Ossicles or petrous bone powdered samples were incubated in 1 mL of lysis buffer (0.45M EDTA and 0.25 mg/mL Proteinase K at pH 8) in screw tubes at 37°C in a rotor incubator. Tooth samples were directly immersed in a lysis buffer (~2–3 mL) in 15 mL centrifuge tubes and incubated under the same conditions as the ossicle and petrous bone samples.

After the lysis buffer was saturated (~18–48 h), we centrifuged the tubes and transferred the supernatants into new clean tubes without disturbing the pellet. An additional 1 mL of lysis buffer (2–3 mL of lysis buffer used for tooth samples) was added onto the tubes and incubated again at 37°C until the buffer saturated. After the second incubation, the tubes were centrifuged at maximum speed, and the supernatants from the two digestion steps for each sample were combined. Next, we added 13 mL of freshly prepared binding buffer (pH 5.2, 5 M guanidine hydrochloride, 40% vol/vol isopropanol, 0.05% Tween-20, and 90 mM sodium acetate) onto the supernatants and filtered the mix through MinElute silica columns (Qiagen). Silica columns were washed twice with a 750 µL PE buffer (Qiagen). At the final step, 50 µL of EB buffer (Qiagen) was added onto the filters in silica columns for DNA elution, and the procedure was repeated twice.

Library preparation and indexing

For libraries prepared in Ankara, we followed the Meyer and Kircher (2010) protocol for preparing Illumina-compatible double-stranded libraries. Blunt-end repair of aDNA fragments was performed with T4 DNA polymerase (Thermo Fisher Scientific), followed by the ligation of adapter oligos to the repaired fragments using T4 DNA Ligase (Thermo Fisher Scientific). Next, the flanking regions of the adapters were filled in using the enzyme Bst polymerase, large fragment (New England Biolabs). We then purified the libraries using the Qiagen MinElute PCR kit. To check the quality of the double-stranded libraries, we performed qPCR analysis. The qPCR Ct values were used to estimate the number of PCR cycles necessary to amplify each library to the threshold value. Each library was amplified and dual-indexed with Illumina-compatible indexes in three 50 µL PCR reactions (Kircher et al. 2012) using AmpliTaq Gold 360 (Thermo Fisher Scientific). From the three PCR products, we collected ~150 µL from each and pooled these together in a single low-binding microcentrifuge tube. To remove primer dimers, nonligated adapters, and long fragments likely to represent modern contamination and to achieve homogeneous fragment sizes, we then cleaned the libraries using AMPure XP beads (Beckman Coulter), sequentially at 0.5× and 1.8× ratios. The concentrations of purified libraries were measured with the Qubit dsDNA high-sensitivity kit. The fragment length and concentration of the libraries were also assessed using an Agilent 2100 Bioanalyzer DNA high-sensitivity kit.

For libraries prepared in Stockholm, we used the single-stranded Santa Cruz reaction protocol (Kapp et al. 2021), with modifications from Nguyen et al. (2023). The libraries were dual-indexed as described above. They were then purified and cleaned using Cytiva beads at specific ratios (0.5× and 1.7×). Library quality was assessed on an Agilent TapeStation with D1000 screen tapes.

For sequencing, libraries with unique index pairs were pooled in equimolar concentrations (final concentration of 10 nM total pool) and sequenced 2 × 150 cycles on Illumina NovaSeq 6000 S1/S4 or NovaSeq X platforms at the National Genomics Infrastructure in Stockholm. Each library was sequenced once.

Data analysis

Data preprocessing and downsampling

Adapter sequences were removed using "*-qualitybase 33 -gzip -trimns*"' parameters using AdapterRemoval (v2.3.3) (Schubert et al. 2016). Paired-end libraries were merged after removing residual adapter sequences, requiring at least 11 bp overlap between the pairs and using additionally "*-collapse -minalignmentlength 11*." The quality of the sequences were studied using the FASTQC software (https://www.bioinformatics.babraham.ac.uk/projects/fastqc/).

We performed the following downsampling scheme to obtain FASTQ files for each library with about 1 million raw reads (including human and nonhuman reads) for comparable estimates of endogenous proportion and clonality, while keeping human mitochondrial DNA reads up to 3× mtDNA coverage in order to obtain reliable contamination estimates using the contamMix software (Fu et al. 2013). First, we mapped reads in the full libraries to the human reference genome (GRCh37) using the "*aln/samse*" algorithm of the Burrows–Wheeler Alignment (BWA) software (v 0.7.15) (Li and Durbin 2009) with the parameters "*-n 0.01, -o 2*" and disabling the seed with "*-l 16500*." We used GRCh37 out of convention, as this genome version has been used as the main human reference in ancient genome studies to date. Although using GRCh38 or T2T would increase proportion of reads mapped, this is not expected to alter the average differences between petrous and ossicle libraries in terms of endogenous proportion or length statistics (Sirak et al. 2020; Mallick et al. 2024). Second, we subsetted the BAM files with reads mapping to the mtDNA using SAMtools software (v 1.18) (Li et al. 2009) with the "*view -b MT*" parameters and then downsampled these up to 3× mitochondrial coverage using SAMtools software (v 1.18) (Li et al. 2009) with the "*view -b -s<fraction_value>*" parameters. Utilizing the read IDs from the resulting files, mitochondrial reads were extracted from the preprocessed FASTQ files using SeqKit software (v2.11.0) (Shen et al. 2024) with the "*grep -f<read_ID_list>*" parameters. This procedure yielded FASTQ files containing exclusively mitochondrial reads, limited to a maximum mitochondrial genome coverage of 3×. Third, we downsampled the preprocessed FASTQ files to 1 million reads using seqtk software (v1.3-r106) (https://github.com/lh3/seqtk/tree/v1.3) with the "*sample -s150 1000000*" parameters. Fourth, to exclude mitochondrial sequences from the downsampled FASTQ files, the data were realigned to the human reference following the same parameters in the first step. Mitochondrial read IDs were then identified using SAMtools (v 1.18) (Li et al. 2009) with the "*view MT*" parameters. Finally, these mitochondrial reads were removed from the downsampled FASTQ files using SeqKit (v2.11.0) (Shen et al. 2024) with the "*grep -v -f<read_ID_list>*" parameters. This procedure resulted in FASTQ files subsampled to 1 million reads, entirely devoid of mitochondrial sequences. Fifth, we merged FASTQ files resulting in the second and fourth steps. We obtained the total number of sequenced reads from these merged FASTQ files. Finally, we realigned the merged FASTQ files to the human reference using the same parameters as in the first step.

Downloaded from genome.cshlp.org on August 3, 2026 . Published by Cold Spring Harbor Laboratory Press

Calculating mapping statistics

We calculated the human proportion using the BAM files obtained as a result of this alignment process. PCR duplicates with identical start and end coordinates were removed using the script "FilterUniqueSAMCons.py" (Kircher 2012). To minimize spurious alignment, reads with alignment quality of less than 30, <35 bp, and containing >10% mismatch were discarded.

After alignment, we calculated the average genome coverage using the genomeCoverageBed algorithm implemented in the bedtools2 software (v2.31.0) (Quinlan and Hall 2010) with reads with a mapping quality >30. The aligned libraries were examined using the PMDtools algorithm with the "*-deamination*" parameter to calculate PMD in DNA (v0.60) (Skoglund et al. 2014). The base position was determined in which the average PMD (cytosine to thymine deamination) at the 5′ ends of reads in each library falls below 1%. The distribution of read lengths and contamination probabilities based on mitochondrial DNA diversity was calculated with the contamMix algorithm using the default parameters (Fu et al. 2013). To ensure the reliability of contamination estimates, the latter analysis was restricted to petrous- and ossicle-matched libraries both having at least 1× mitochondrial DNA coverage (contamMix estimates become unreliable below this range).

To determine the human endogenous DNA content of each obtained library, we used the ratio of the sequences (i.e., merged reads) aligned to the human reference genome to all sequences in that library. We used the filtered sequences (as described above) but without removing duplicates (because technical factors such as higher PCR cycles or sequencing depth will increase duplication levels).

To calculate mean fragment lengths for raw reads from FASTQ files, we used SeqKit (v2.11.0) (Shen et al. 2024) software with the "*stats -T*" parameters. For mapped reads, we used SAMtools with a "*-q 30*" filter to obtain the distribution of fragment lengths from BAM files. We then calculated the mean fragment length for each BAM file using an in-house bash script (see Supplemental Code). Mean fragment length distributions of raw (FASTQ) and mapped (BAM) reads for libraries from each tissue type are summarized in Supplemental Figure 2.

To estimate the percentage of clonality, which we define as the proportion of duplicate reads to total reads, was calculated for each BAM file using the same procedure described above.

Metagenomic analysis

For metagenomic screening, we followed the aMeta pipeline (Pochon et al 2023) up to the KrakenUniq step. FASTQ files for each library were screened for microbial reads using the KrakenUniq (v1.0.4) (Breitwieser et al. 2018) database provided by aMeta, which includes NCBI nonredundant NT/NR records (June 2020) comprising archaea, bacteria, viruses, fungi, protozoa, parasitic worms, humans, and several complete eukaryotic genomes (Pochon et al. 2023). KrakenUniq results were filtered by retaining taxa with at least 100 unique *k*-mers and 10 unique reads. Microbial source data were obtained from three databases: Expanded Human Oral Microbiome Database (eHOMD v4.1) (Escapa et al. 2018), Bac*Dive* Database (Schober et al. 2025), and MicrobeAtlas Database (Matias Rodrigues et al. 2026). Using a custom R script (see Supplemental Code), microbial species were classified as originating from human, oral, or nonoral sources. Relative abundances were calculated by dividing the number of reads assigned to each microbial species/source by the total number of microbial species/source reads assigned to any species in the individual library by KrakenUniq.

Statistical analyses

All statistical analyses were conducted in R (R Core Team 2025). We used the packages readxl (https://CRAN.R-project.org/package=readxl), tidyverse (Wickham et al. 2019), and reshape2 (Wickham 2007) for data processing. WSR tests were performed using the wilcox.test function from the R *stats* package (R Core Team 2025). Pairwise comparisons were performed using MWU tests via the pairwise.wilcox.test function in the R *stats* package (R Core Team 2025). To control the false-discovery rate, *P*-values were adjusted using the Benjamini–Hochberg method (*P*.adj = "BH"). Visualizations were created using ggplot2 (Wickham 2016), ggtern (Hamilton and Ferry 2018), superb (Cousineau et al. 2021), rnaturalearth (https://CRAN.R-project.org/package=rnaturalearth), raster (https:// CRAN.R-project.org/package=raster), ggrepel (https://CRAN.R-project.org/package=ggrepel), ggpubr (https://cran.r-project.org/web/packages/ggpubr), ggforce (https://CRAN.R-project.org/package=ggforce), ggbeeswarm (https://CRAN.R-project.org/package=ggbeeswarm), png (https://CRAN.R-project.org/package=png), grid (R Core Team 2025), ggh4x (https://CRAN.R-project.org/package=ggh4x), and *DescTools* (https://cran.r-project.org/web/packages/DescTools) R packages.

Ethical considerations

All samples used in this study are archaeological/historical specimens older than 200 years and therefore are not considered human-subject research under current ethical and legal frameworks. As such, institutional ethical approval was not required. The specimens were obtained from authorized collections through the relevant museum/curatorial authorities, and all permissions for sampling, destructive analysis, and publication were granted prior to the study. No modern individuals or identifiable personal data were involved. All work was conducted in accordance with the ethical guidelines for the study of historical human remains of the country of origin.

Code availability

All custom codes related to the statistical analyses of this project are available at GitHub (https://github.com/ardasevkar/Auditory-Ossicles) and as Supplemental Code.

Data access

The DNA sequence data generated in this study have been submitted to the European Nucleotide Archive (ENA; https://www.ebi.ac.uk/ena/browser/) under the accession number PRJEB108518.

Competing interest statement

The authors declare no competing interests.

Acknowledgments

We thank members of the CompEvo (METU), HUMAN_G (Hacettepe University), and Archaegenetics (CPG) groups; Eva-Maria Geigl, Thierry Grange, Vendela Kempe Lagerholm, Dilek Koptekin, N. Ezgi Altınışık, Hannah M. Moots, Tom Booth, and Reyhan Yaka for support and/or helpful suggestions; and Ron Pinhasi and two anonymous reviewers for their constructive comments. This work was supported by the H2020 ERC Consolidator grant (no. 772390 NEOGENE to M.S.) and the H2020-WIDESPREAD-05-2020 TWINNING grant (no. 952317 NEOMATRIX to M.S.). E.S. was supported by the Council of Higher Education of Turkey (YÖK 100/2000 PhD Scholarship).

Downloaded from genome.cshlp.org on August 3, 2026 . Published by Cold Spring Harbor Laboratory Press

A.S. was supported by the Scientific and Technological Research Council of Türkiye (TÜBİTAK BİDEB 2211-A National PhD Scholarship Program). G.O.G. was funded by the European Union's Horizon 2020 research and innovation program under grant agreement no. 101034324. M.S. was supported by the VR Center of Excellence, the Center for the Human Past under the Swedish Research Council grant no. 2022-06620_VR, and a Wenner-Gren Stiftelserna Visiting Research Fellowship (GFOh2024-0045).

References

Bell LS, Kayser M, Jones C. 2008. The mineralized osteocyte: a living fossil. *Am J Phys Anthropol* **137:** 449–456. doi:10.1002/ajpa.20886

Breitwieser FP, Baker DN, Salzberg SL. 2018. KrakenUniq: confident and fast metagenomics classification using unique *k*-mer counts. *Genome Biol* **19:** 198. doi:10.1186/s13059-018-1568-0

Bruintjes TD, Panhuysen RGAM, Van Maurik WAM. 1997. An unusual stapes from medieval Maastricht. *Int J Osteoarchaeol* **7:** 641–642. doi:10.1002/(SICI)1099-1212(199711/12)7:6%253C641::AID-OA312%253E3.0.CO;2-X

Cousineau D, Goulet M-A, Harding B. 2021. Summary plots with adjusted error bars: the superb framework with an implementation in R. *Adv Methods Pract Psychol Sci* **4:** 25152459211035109. doi:10.1177/25152459211035109

Dabney J, Knapp M, Glocke I, Gansauge MT, Weihmann A, Nickel B, Valdiosera C, García N, Pääbo S, Arsuaga JL, et al. 2013. Complete mitochondrial genome sequence of a middle Pleistocene cave bear reconstructed from ultrashort DNA fragments. *Proc Natl Acad Sci* **110:** 15758–15763. doi:10.1073/pnas.1314445110

Escapa IF, Chen T, Huang Y, Gajare P, Dewhirst FE, Lemon KP. 2018. New insights into human nostril microbiome from the expanded Human Oral Microbiome Database (eHOMD): a resource for the microbiome of the human aerodigestive tract. *mSystems* **3:** e00187-18. doi:10.1128/msystems.00187-18

Frisch T, Sørensen MS, Overgaard S, Lind M, Bretlau P. 1998. Volume-referent bone turnover estimated from the interlabel area fraction after sequential labeling. *Bone* **22:** 677–682. doi:10.1016/S8756-3282(98)00050-7

Fu Q, Mittnik A, Johnson PLF, Bos K, Lari M, Bollongino R, Sun C, Giemsch L, Schmitz R, Burger J, et al. 2013. A revised timescale for human evolution based on ancient mitochondrial genomes. *Curr Biol* **23:** 553–559. doi:10.1016/J.CUB.2013.02.044

Gamba C, Jones ER, Teasdale MD, McLaughlin RL, Gonzalez-Fortes G, Mattiangeli V, Domboróczki L, Kővári I, Pap I, Anders A, et al. 2014. Genome flux and stasis in a five millennium transect of European prehistory. *Nat Commun* **5:** 5257. doi:10.1038/ncomms6257

Gaudio D, Fernandes DM, Schmidt R, Cheronet O, Mazzarelli D, Mattia M, O'Keeffe T, Feeney RNM, Cattaneo C, Pinhasi R. 2019. Genome-Wide DNA from degraded petrous bones and the assessment of sex and probable geographic origins of forensic cases. *Sci Rep* **9:** 8226. doi:10.1038/s41598-019-44638-w

Haarkötter C, Vinueza-Espinosa DC, Gálvez X, Saiz M, Medina-Lozano MI, Lorente JA, Álvarez JC. 2023. A comparison between petrous bone and tooth, femur and tibia DNA analysis from degraded skeletal remains. *Electrophoresis* **44:** 1559–1568. doi:10.1002/elps.202300097

Hamilton NE, Ferry M. 2018. ggtern: ternary diagrams using ggplot2. *J Stat Softw*, Code Snippets **87:** 1–17. doi:10.18637/jss.v087.c03

Hansen HB, Damgaard PB, Margaryan A, Stenderup J, Lynnerup N, Willerslev E, Allentoft ME. 2017. Comparing ancient DNA preservation in petrous bone and tooth cementum. *PLoS One* **12:** e0170940. doi:10.1371/journal.pone.0170940

Hofreiter M, Sneberger J, Pospisek M, Vanek D. 2021. Progress in forensic bone DNA analysis: lessons learned from ancient DNA. *Forensic Sci Int Genet* **54:** 102538. doi:10.1016/j.fsigen.2021.102538

Ibrahim J, Brumfeld V, Addadi Y, Rubin S, Weiner S, Boaretto E. 2022. The petrous bone contains high concentrations of osteocytes: one possible reason why ancient DNA is better preserved in this bone. *PLoS One* **17:** e0269348. doi:10.1371/journal.pone.0269348

Ivanovic A, Schalbetter F, Schmeltz M, Wimmer W, Caversaccio M, Stampanoni M, Bonnin A, Anschuetz L. 2024. Characterizing bone density pattern and porosity in the human ossicular chain using synchrotron microtomography. *Sci Rep* **14:** 18498. doi:10.1038/s41598-024-69608-9

Kapp JD, Green RE, Shapiro B. 2021. A fast and efficient single-stranded genomic library preparation method optimized for ancient DNA. *J Hered* **112:** 241–249. doi:10.1093/jhered/esab012

Kircher M. 2012. Analysis of high-throughput ancient DNA sequencing data. *Methods Mol Biol* **840:** 197–228. doi:10.1007/978-1-61779-516-9_23

Kircher M, Sawyer S, Meyer M. 2012. Double indexing overcomes inaccuracies in multiplex sequencing on the Illumina platform. *Nucleic Acids Res* **40:** e3. doi:10.1093/NAR/GKR771

Leskovar T, Beaumont J, Lisić N, McGalliard S. 2019. Auditory ossicles: a potential biomarker for maternal and infant health *in utero*. *Ann Hum Biol* **46:** 367–377. doi:10.1080/03014460.2019.1639824

Li H, Durbin R. 2009. Fast and accurate short read alignment with Burrows–Wheeler transform. *Bioinformatics* **25:** 1754–1760. doi:10.1093/BIOINFORMATICS/BTP324

Li H, Handsaker B, Wysoker A, Fennell T, Ruan J, Homer N, Marth G, Abecasis G, Durbin R, 1000 Genome Project Data Processing Subgroup. 2009. The Sequence Alignment/Map format and SAMtools. *Bioinformatics* **25:** 2078–2079. doi:10.1093/BIOINFORMATICS/BTP352

Lisoněk P, Kutal M, Peške L, Kubinek R. 1986. Auditory ossicles from archaeological finds. *Anthropologie (1962-)* **24:** 185–188.

Mallick S, Micco A, Mah M, Ringbauer H, Lazaridis I, Olalde I, Patterson N, Reich D. 2024. The Allen Ancient DNA Resource (AADR) a curated compendium of ancient human genomes. *Sci Data* **11:** 182. doi:10.1038/s41597-024-03031-7

Margaryan A, Hansen HB, Rasmussen S, Sikora M, Moiseyev V, Khoklov A, Epimakhov A, Yepiskoposyan L, Kriiska A, Varul L, et al. 2018. Ancient pathogen DNA in human teeth and petrous bones. *Ecol Evol* **8:** 3534–3542. doi:10.1002/ece3.3924

Marotti G, Farneti D, Remaggi F, Tartari F. 1998. Morphometric investigation on osteocytes in human auditory ossicles. *Ann Anat* **180:** 449–453. doi:10.1016/S0940-9602(98)80106-4

Matias Rodrigues JF, Tackmann J, Malfertheiner L, Patsch D, Perez-Molphe-Montoya E, Näpflin N, Gaio D, Rot G, Danaila M, Peluso ME, et al. 2026. The MicrobeAtlas database: global trends and insights into Earth's microbial ecosystems. *Cell* **189:** 2092–2107.e17. doi:10.1016/j.cell.2026.01.021

Meyer M, Kircher M. 2010. Illumina sequencing library preparation for highly multiplexed target capture and sequencing. *Cold Spring Harb Protoc* **2010:** pdb.prot5448. doi:10.1101/PDB.PROT5448

Nguyen R, Kapp JD, Sacco S, Myers SP, Green RE. 2023. A computational approach for positive genetic identification and relatedness detection from low-coverage shotgun sequencing data. *J Hered* **114:** 504–512. doi:10.1093/jhered/esad041

Parker C, Rohrlach AB, Friederich S, Nagel S, Meyer M, Krause J, Bos KI, Haak W. 2020. A systematic investigation of human DNA preservation in medieval skeletons. *Sci Rep* **10:** 18225. doi:10.1038/s41598-020-75163-w

Pinhasi R, Fernandes D, Sirak K, Novak M, Connell S, Alpaslan-Roodenberg S, Gerritsen F, Moiseyev V, Gromov A, Raczky P, et al. 2015. Optimal ancient DNA yields from the inner Ear part of the human petrous bone. *PLoS One* **10:** e0129102. doi:10.1371/JOURNAL.PONE.0129102

Pinhasi R, Fernandes DM, Sirak K, Cheronet O. 2019. Isolating the human cochlea to generate bone powder for ancient DNA analysis. *Nat Protoc* **14:** 1194–1205. doi:10.1038/s41596-019-0137-7

Pochon Z, Bergfeldt N, Kırdök E, Vicente M, Naidoo T, van der Valk T, Altınışık NE, Krzewińska M, Dalén L, Götherström A, et al. 2023. aMeta: an accurate and memory-efficient ancient metagenomic profiling workflow. *Genome Biol* **24:** 242. doi:10.1186/s13059-023-03083-9

Ponce de León MS, Koesbardiati T, Weissmann JD, Milella M, Reyna-Blanco CS, Suwa G, Kondo O, Malaspinas A-S, White TD, Zollikofer CPE. 2018. Human bony labyrinth is an indicator of population history and dispersal from Africa. *Proc Natl Acad Sci* **115:** 4128–4133. doi:10.1073/pnas.1717873115

Prendergast ME, Lipson M, Sawchuk EA, Olalde I, Ogola CA, Rohland N, Sirak KA, Adamski N, Bernardos R, Broomandkhoshbacht N, et al. 2019. Ancient DNA reveals a multistep spread of the first herders into sub-saharan Africa. *Science* **365:** eaaw6275. doi:10.1126/science.aaw6275

Quinlan AR, Hall IM. 2010. BEDTools: a flexible suite of utilities for comparing genomic features. *Bioinformatics* **26:** 841–842. doi:10.1093/BIOINFORMATICS/BTQ033

Qvist M. 2000. Auditory ossicles in archaeological skeletal material from medieval Denmark. *Acta Otolaryngol* **120:** 82–85. doi:10.1080/000164800454053

R Core Team. 2025. *R: a language and environment for statistical computing*. R Foundation for Statistical Computing, Vienna. https://www.R-project.org/.

Richard C, Courbon G, Laroche N, Prades JM, Vico L, Malaval L. 2017. Inner ear ossification and mineralization kinetics in human embryonic development: microtomographic and histomorphological study. *Sci Rep* **7:** 4825. doi:10.1038/s41598-017-05151-0

Rolvien T, Stürznickel J, Schmidt FN, Butscheidt S, Schmidt T, Busse B, Mundlos S, Schinke T, Kornak U, Amling M, et al. 2018. Comparison of bone microarchitecture between adult osteogenesis imperfecta and

Downloaded from genome.cshlp.org on August 3, 2026 . Published by Cold Spring Harbor Laboratory Press

early-onset osteoporosis. *Calcif Tissue Int* **103:** 512–521. doi:10.1007/s00223-018-0447-8

Sakalinskas V, Jankauskas R. 1991. An otological investigation of Lithuanian skulls. *Int J Osteoarchaeol* **1:** 127–134. doi:10.1002/oa.1390010208

Schober I, Koblitz J, Sardà Carbasse J, Ebeling C, Schmidt ML, Podstawka A, Gupta R, Ilangovan V, Chamanara J, Overmann J, et al. 2025. Bac*Dive* in 2025: the core database for prokaryotic strain data. *Nucleic Acids Res* **53:** D748–D756. doi:10.1093/nar/gkae959

Schubert M, Lindgreen S, Orlando L. 2016. AdapterRemoval v2: rapid adapter trimming, identification, and read merging. *BMC Res Notes* **9:** 88. doi:10.1186/s13104-016-1900-2

Schwark T, Modrow J-H, Steinmeier E, Poetsch M, Hasse J, Fischer H, von Wurmb-Schwark N. 2015. The auditory ossicles as a DNA source for genetic identification of highly putrefied cadavers. *Int J Legal Med* **129:** 457–462. doi:10.1007/s00414-015-1177-3

Shen W, Sipos B, Zhao L. 2024. Seqkit2: a Swiss army knife for sequence and alignment processing. *iMeta* **3:** e191. doi:10.1002/imt2.191

Sikora M, Canteri E, Fernandez-Guerra A, Oskolkov N, Ågren R, Hansson L, Irving-Pease EK, Mühlemann B, Holtsmark Nielsen S, Scorrano G, et al. 2025. The spatiotemporal distribution of human pathogens in ancient Eurasia. *Nature* **643:** 1011–1019. doi:10.1038/s41586-025-09192-8

Sirak K, Fernandes D, Cheronet O, Harney E, Mah M, Mallick S, Rohland N, Adamski N, Broomandkhoshbacht N, Callan K, et al. 2020. Human auditory ossicles as an alternative optimal source of ancient DNA. *Genome Res* **30:** 427–436. doi:10.1101/gr.260141.119

Skoglund P, Northoff BH, Shunkov MV, Derevianko AP, Pääbo S, Krause J, Jakobsson M. 2014. Separating endogenous ancient DNA from modern day contamination in a Siberian Neandertal. *Proc Natl Acad Sci* **111:** 2229–2234. doi:10.1073/PNAS.1318934111

Sørensen MS, Jørgensen MB, Bretlau P. 1992. Drift barriers in the postcartilaginous development of the mammalian otic capsule. *Eur Arch Otorhinolaryngol* **249:** 56–61. doi:10.1007/BF00175673

Wickham H. 2007. Reshaping data with the reshape package. *J Stat Softw* **21:** 1–20. doi:10.18637/JSS.V021.I12

Wickham H. 2016. *ggplot2: elegant graphics for data analysis*. Springer-Verlag, New York. https://ggplot2.tidyverse.org.

Wickham H, Averick M, Bryan J, Chang W, McGowan LD, François R, Grolemund G, Hayes A, Henry L, Hester J, et al. 2019. Welcome to the tidyverse. *J Open Source Softw* **4:** 1686. doi:10.21105/joss.01686

Zupanič Pajnič I, Jeromelj T, Leskovar T. 2025. Petrous bones versus tooth cementum for genetic analysis of aged skeletal remains. *Int J Legal Med* **139:** 41–48. doi:10.1007/s00414-024-03346-5

Received July 17, 2025; accepted in revised form June 5, 2026.